Quantitative graphical description of portocentral gradients in hepatic gene expression by image analysis

Lamers, W.H.; Geerts, W.J.C.; Jonker, A.; Verbeek, F.J.; Wagenaar, G.T.M.; Moorman, A.F.M.

Publication date
1997

Published in
Hepatology

Quantitative Graphical Description of Portocentral Gradients in Hepatic Gene Expression by Image Analysis

WOUTER H. LAMERS, WILLIE J. C. GEERTS, ARD JONKER, FONS J. VERBEEK, GERRY T. M. WAGENAAR, AND ANTOON F. M. MOORMAN

The liver consists of numerous repeating, randomly oriented, more or less cylindrical units, the lobules. Although enzyme-histochemical or microbiochemical assays accurately reflect zonal differences in lobular enzyme content, their results cannot be directly compared to biochemical assays. This is because section-based assays typically sample along a linear portocentral column of cells, even though periportal regions contribute substantially more to hepatic volume than pericentral regions. We have developed a time-efficient approach that depends on image analysis to determine the prevalence of hepatocytes (pixels) with a defined cellular concentration of a particular gene product (absorbance), and that generates a graph with the average absorbance per hepatocyte on the ordinate and the percentage of hepatocytes with absorbances in each of a predetermined range of absorbances incrementally summed on the abscissa. The direction of the gradient is read directly from the section. The gradient is a graphical representation of the two-dimensional distribution pattern of the gene product between the portal tracts and the central veins. The total surface area underneath the resulting graph represents the integrated absorbance and is equivalent to the outcome of a biochemical assay. The typical linear portocentral gradient can be derived from that representing the two-dimensional distribution if we assume that liver lobules are uniformly cylindrical or prismatic. The analysis, therefore, yields a quantitative description of the relation between the enzymatic phenotype of hepatocytes and their position on a normalized portocentral radius. We have used the procedure to compare portocentral gradients of different enzymes in the same liver and of the same enzyme in different livers. In addition, bipolar portocentral gradients of the same enzyme in the same liver were analyzed. (HEPATOLOGY 1997;26:398-406.)

The liver is a perfect example of an organ that consists of numerous small, repeating units. The liver shares this structural property with many other metabolically important organs, such as the intestines (villi) and the kidneys (nephrons). The repetitive nature of the unit structure makes such organs the organs of choice to study the molecular mechanisms underlying metabolic regulation but also underscores the importance of a proper understanding of structure-function relationships within these units. Using differences in the cellular concentration of enzymes as a parameter, two subpopulations of hepatocytes can be recognized, those around the branches of the portal vein (periportal hepatocytes) and those around the branches of the hepatic vein (pericentral hepatocytes). Many aspects of hepatic metabolism can only be understood in the context of the mostly complementary functions of the hepatocytes in the periportal and pericentral zones of the liver.[1-3] The distribution patterns of enzymes in conjunction with the angioarchitecture[4] and the perfusion pattern[5,6] of the liver show that the hepatic lobule (as opposed to the hepatic acinus[7,8]) is the smallest repeating structural unit of a normal liver. The most important structural feature of the hepatic lobule is that the central vein represents its longitudinal axis, while the terminal branches of the portal vein form its periphery.

Despite the simple geometry of the hexagonal array of liver lobules that is usually presented in textbooks, it is not yet possible to directly relate enzyme-histochemical or microbiochemical measurements to more classical biochemical assays in homogenates, because the relative contribution of the periportal and pericentral cells to the total make-up of the hepatocyte population in the liver is not taken into account. This is because most section-based assays are based on sampling of hepatocytes along the linear portocentral radius (the average distance along the hepatic sinusoids between the portal tracts and the central veins, which in rat liver is reported to be 300 to 450 μm long[9-12]), whereas in reality, hepatocytes are clustered into polygonal domains representing cross sections through the lobules (Fig. 1). The periportal hepatocytes occupy the periphery of the polygons, whereas the pericentral cells occupy their center, i.e., the periportal cells contribute significantly more to the surface area of the section than the pericentral cells. For example, it can easily be calculated that microbiochemical assays of rat liver, performed on rectangular portocentral strips of 400 μm and partitioned in 10 pieces of equal length, underestimate the total contribution of the most peripheral layer of periportal cells to hepatic enzyme content by twofold (this layer occupies 20% of the surface area and 10% of the portocentral radius of a lobule) and overestimate the contribution of the most centrally localized layer of pericentral cells by 10-fold (this layer occupies 1% of the surface area and 10% of the portocentral radius in this example). To relate section-based assays to assays based on tissue homogenates, it is

Abbreviations: mRNA, messenger RNA; CPS, carbamoylphosphate synthetase; GS, glutamine synthetase; PEP-CK, phosphoenolpyruvate carboxykinase; GDH, glutamate dehydrogenase.

From the Department of Anatomy and Embryology, Academic Medical Center, University of Amsterdam, The Netherlands.

Received November 7, 1996; accepted March 7, 1997.

Address reprint requests to: W. H. Lamers, M.D., Ph.D., Department of Anatomy and Embryology, Academic Medical Center, Meibergdreef 15, 1105 AZ Amsterdam, The Netherlands. Fax: 31-20-697-6177.

0270-9139/97/2602-0022$3.00/0

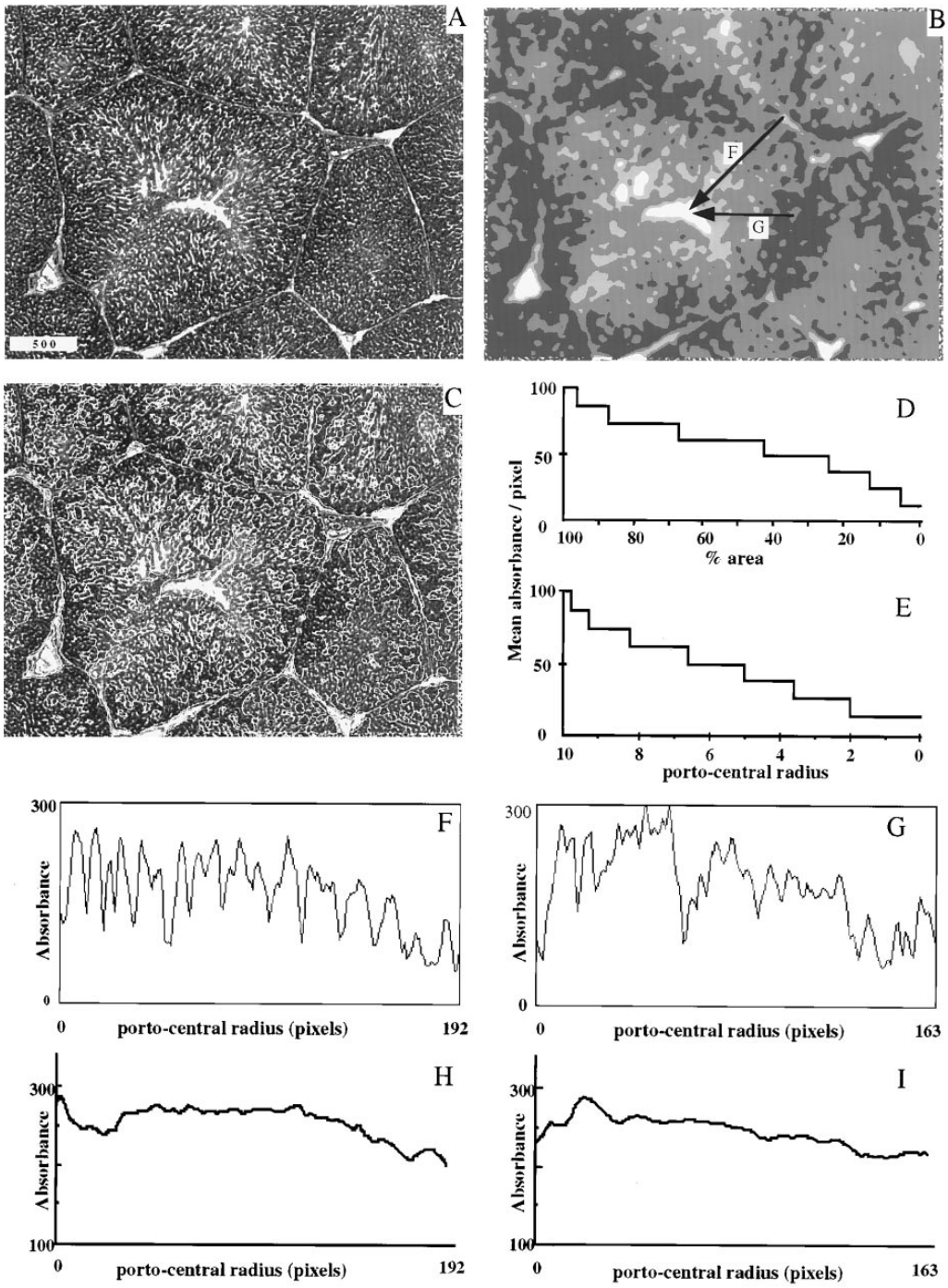

FIG. 1. Expression pattern of CPS protein in adult porcine liver. (A) A digital image of an immunohistochemically stained section. (B) The same image after application of a Gaussian filter, subtraction of the background signal that is observed over the connective tissue of the portal tracts, and subdivision of the remaining hepatocyte-specific absorbance into a high, an intermediate, and a low range. (C) The jagged contours observed in panel B are superimposed on (A) to show that it follows cellular contours. (D) The frequency distribution of the number of pixels overlying hepatocytes in successive absorbance ranges after dividing the total range between the highest and lowest specific absorbance over hepatocytes into equal portions. By serially arranging these absorbance ranges in an ascending or descending order, i.e., according to the *a priori* knowledge of the direction of the portocentral gradient, the frequency distribution profile of pixels overlying hepatocytes with a particular absorbance in such a section is obtained. (D) is therefore a graphical representation of the two-dimensional distribution pattern of CPS along the portocentral radius. (E) The linear portocentral gradient in the content of CPS and is obtained by recalculating the data from panel D as detailed in Materials and Methods, assuming that the liver is made up of uniform cylindrical lobules with the central vein as their longitudinal axis. (F-I) The absorbance along the portocentral radius indicated by the lines in (B) is shown before (F and G) and after (H and I) smoothing by determining the moving average of 11 pixels. (D-I) The portal tracts are located at the left end of the abscissa and the central veins on the right end. *Bar* = 500 μm.

necessary to use a truly two-dimensional sampling method. In this respect, Teutsch was the first to develop a sampling method that used wedge-shaped rather than rectangular strips.[11] However, this approach requires three-dimensional computer graphics for a proper imaging of the distribution of the parameters investigated[13,14] and, therefore, complicates a rapid and simple comparison of the distribution of different parameters.

Another potentially important implication of the lobular architecture of the liver is that the enzymic make-up of a hepatocyte can be predicted from its position on the portocentral radius. That simplified description of the functional capacity of a complex three-dimensional organ to a one-dimensional parameter is obviously very relevant for mathematical modeling of liver metabolism but requires an estimation of the size and shape of the lobular unit. If the lobule would be a more or less cylindrical or prismatic structure, the position of the hepatocyte on the portocentral radius could indeed be read directly from the section. Tacitly accepting this assumption, gradients are usually expressed by assigning samples according to their location; thus, the midpoints of microdissected samples are related to their distance from the central vein[10,11] or to their relative position on the portocentral radius.[15,16] However, lobules are tortuous, branching structures with a ratio of axial length to diameter of approximately 3[17] (W.H.L., unpublished observations).

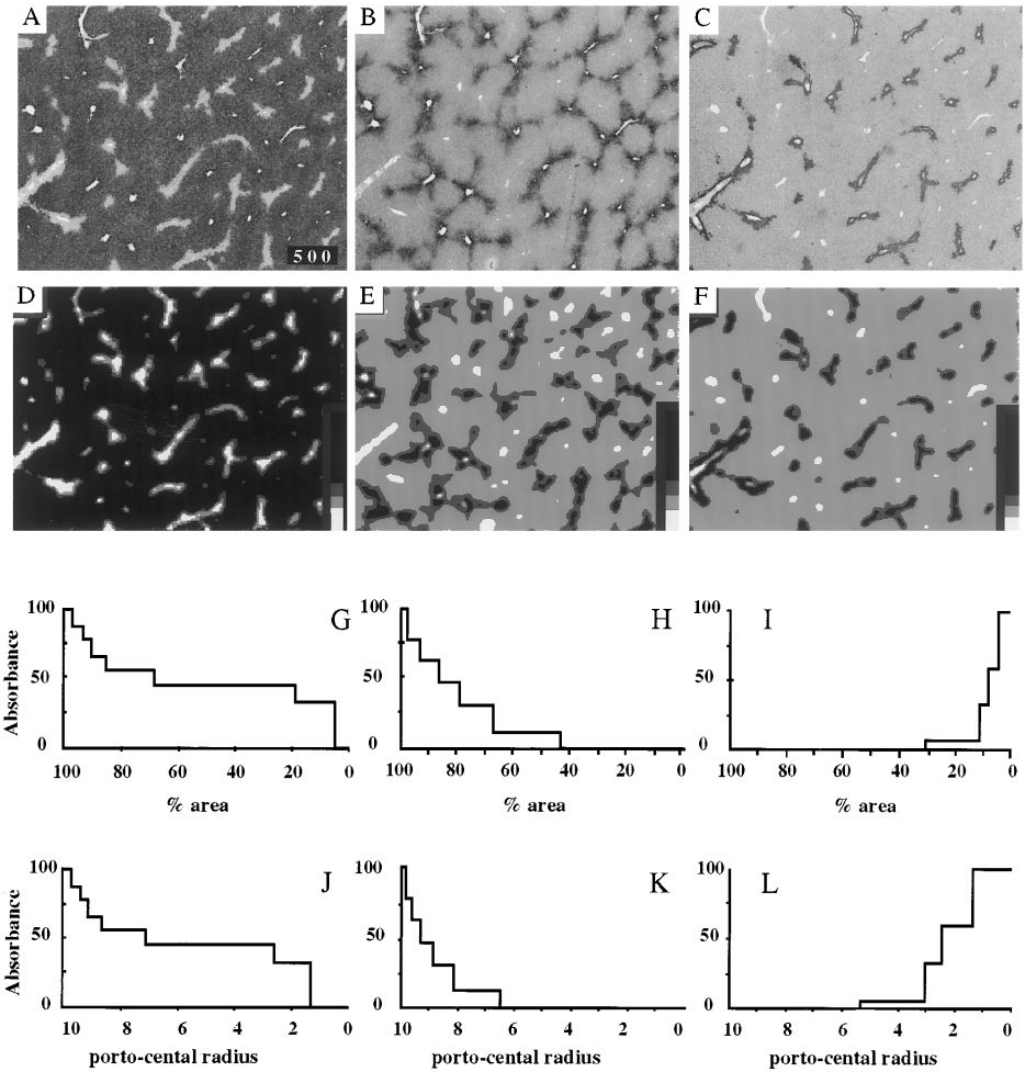

FIG. 2. Expression pattern of CPS protein (A, D, G, and J), PEPCK protein (B, E, H, and K), and GS protein (C, F, I, and L) in adult mouse liver. (A-C) Digital images of immunohistochemically stained sections. (D-F) The same series of images after subdividing the hepatocyte-specific absorbance into a high, an intermediate, and a low range. (G-I) The frequency distribution of the number of pixels overlying hepatocytes in each of a number of successive absorbance ranges after dividing the total range between the highest and lowest specific absorbance over hepatocytes into equal portions. (G-I) A graphical representation of the two-dimensional distribution pattern of the three enzymes along the portocentral radius as shown in the images of panels (A-C). (J-L) The linear portocentral gradient in the content of the respective enzymes, obtained by recalculating the data from panels G-I as detailed in Materials and Methods, assuming that the liver is made up of uniform cylindrical lobules with the central vein as their longitudinal axis. (G-L) The portal tracts are located at the left end of the abscissa and the central veins on the right end. *Bar* = 500 μm.

These structural features explain why truly sagittal or transverse sections of a lobule are extremely rare. Furthermore, it can be shown that in sections, the position of a midlobular sample in such a tortuous lobule will appear to have moved towards the portal or central extremity of the portocentral radius, depending on the local direction of the curvature. It is, therefore, necessary to develop procedures to calculate the course of portocentral gradients from sections that do not depend on the plane of section with respect to the local geometry of a particular lobule.

We have developed an analytical approach to calculate the frequency distribution of hepatocytes with quantitatively the same staining intensity (enzymic phenotype) within a section or series of sections. That approach, therefore, depends on the specificity of staining of hepatocytes, i.e., on the hepatocyte-specific expression of the gene under study. In connection with knowledge of the general direction of the gradient in hepatocellular enzyme or messenger RNA (mRNA) content, the method allows one to assess the steepness of the portocentral gradient of the concentration of this compound without simultaneous measurement of the portocentral radii. A further advantage of the approach is that the frequency distribution of hepatocytes with quantitatively the same phenotype can be directly related to biochemical measurements in total tissue homogenates.

MATERIALS AND METHODS

Staining Procedures. Examples were taken from previous studies as indicated. Immunohistochemical localization of enzyme proteins was performed on methanol/acetone/water (2:2:1 vol:vol:vol)-fixed tissue, using the indirect unconjugated peroxidase-antiperoxidase technique with 3,3′-diaminobenzidine and H_2O_2 as substrates to visualize the distribution patterns.[18] *In situ* hybridization with ^{35}S-labeled complementary RNA probes was performed on buffered 4% formaldehyde-fixed tissue as described.[19,20] Absorbance measurements of immunohistochemical and hybridization signals on sections reflect cellular protein and mRNA levels, respectively, if processed under well-defined and strictly comparable conditions.[20-22] Initial reaction rates of glutamate dehydrogenase enzyme activity were determined on unfixed cryostat sections, using glutamate-dependent formazan production as parameter.[23,24]

Image Recording and Analysis. Images of liver sections were recorded as described.[24] Briefly, we used a Photometrics cooled charge-coupled device (CCD) camera (Photometrics, Tucson, AZ) (12-bit dynamic range; 1317*1035 pixels) attached to an Axioplan microscope (Zeiss, Oberkochen, Germany) and equipped with a ×2.5 objective (numerical aperture: 0.075), a stabilized power supply and an infrared-blocking filter. The low-power objective was

used to assure the sampling of several lobules in an image. Tissue-mRNA expression (silver grains) was recorded using white light,[20] enzyme protein (oxidized diaminobenzidine) was recorded at 480 nm, and enzyme activity (nitroblue-formazan precipitate) was recorded at 585 nm. Digital images (3.4*2.8 mm) were corrected for background shading by transformation into density (mRNA) or absorbance images (enzyme protein and activity). Calculations on absorbances and densities were performed identically.[25] Image analysis was performed on a SUN Sparc 1^+ computer and a Macintosh Power PC. The SCIL-IMAGE image processing functions[26] and the public domain NIH Image Program (developed at the US National Institutes of Health and available on the Internet at http://rsb.info.nih.gov/nih-image/) was used to measure the distribution of absorbances. A home-made macro was used for determination of the absorbance slices.

Graphical Representation of Distribution Patterns. To remove sinusoidal spaces, which occupy an average of 5 pixels, the images were smoothed by applying a Gaussian filter with s_x and s_y of 5 pixels. After this preprocessing, the level of gene expression (absorbance) and the position of the cell on the portocentral radius showed an excellent topographical correlation (Figs. 1 and 2). Background absorbance was determined in the connective tissue of the portal tracts and subtracted from the original absorbance image of the section to obtain an image representing the specific absorbance in hepatocytes. After determining the highest and lowest absorbances in the resulting image, the absorbance range was subdivided in 10 grey-value ranges, each representing 10% of the hepatocyte-specific absorbance intensity range. Next, the number of pixels with absorbance values corresponding to each of the 10 grey-value ranges, i.e., the surface area of each of the grey-value ranges, was determined. Data were imported into a Microsoft Excel™ (Irvine, CA) spreadsheet. The percent area occupied by each grey-value range and the average absorbance per pixel in this grey-value range were calculated. These average absorbances were serially arranged in an ascending or descending order, i.e., according to the *a priori* knowledge of the direction of the portocentral gradient. When the area of a particular grey-value range occupied <3% of the total area measured, which corresponds to approximately one layer of cells in the pericentral zone (see below) and which occurred only in the highest grey-value ranges, it was added to the neighboring grey-value range, followed by recalculation of the average absorbance per pixel. Finally, a graph was constructed with the average absorbance per pixel in the respective grey-value ranges represented on the ordinate and the percentage of pixels overlying hepatocytes with absorbances/densities in each of the predetermined grey-value ranges incrementally summed on the abscissa. The total surface area underneath the resulting graph therefore represents the integrated absorbance overlying the hepatocytes. The position of the portal tract is always depicted on the left end of the abscissa of these graphs and on the central vein on the right end, irrespective of whether the highest or the lowest grey-value range overlays it. However, as detailed in the introduction, portocentral gradients in gene expression are normally related to the portocentral radius (r) rather than to the surface area occupied by differentially stained periportal and pericentral cells. The frequency distribution pattern, described previously, applies to the portion of the section surface occupied by hepatocytes. Assuming that the hepatic lobule can be represented as a cylinder or a prism (cross-sectional area $\sim r^2$), the position on the portocentral radius of hepatocytes with a specific grey-value range can be approximated by taking the square root of the area of the corresponding surface. When applying this calculation, it should be kept in mind that the central vein is the longitudinal radius of the lobule, and the distributing branches of the portal vein represent its periphery (e.g., Fig. 1). Furthermore, because the central vein forms the axis of the lobule and because the proposed calculation involves a square root, a serious distortion of the calculated position of the pericentral hepatocytes on the portocentral radius develops if the surface area of the central vein is not taken into account (Fig. 3). We have estimated the diameter of the average central vein to be the equivalent of three hepatocytes, or approximately 2% of the surface area of a lobule. We used the following formula to approximate the relative position (P) on the portocentral radius of a hepatocyte having an absorbance within a specified range, as a function of the percentage of the section surface area (A) occupied by the hepatocytes characterized by that absorbance range:

$$P(A) = 10\sqrt{A\text{-}a} \div \sqrt{100\text{-}a}.$$

The "a" refers to the percentage of the section surface area occupied by the central veins.

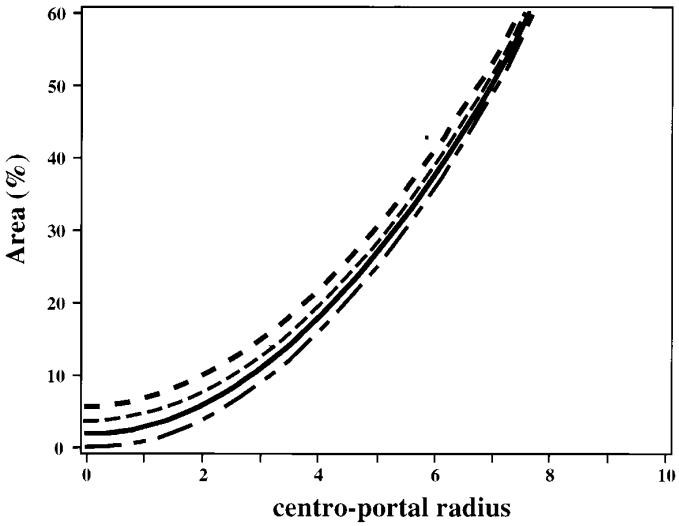

FIG. 3. Influence of the surface area of the central vein on the calculated position of a hepatocyte with a specified absorbance on the portocentral radius. The relation between the area occupied by hepatocytes with a specified absorbance (vertical axis) and the position of these hepatocytes on the portocentral radius (horizontal axis) is calculated by taking the square root of the area as indicated in the text. Depending on the size of the central veins (occupying 0%(Δ), 1%(◆), 2%(□), or 3%(○) of the section in this example), the calculated position of a hepatocyte with a specified absorbance changes along the portocentral radius as shown.

Bipolar Portocentral Gradients. Description of bipolar portocentral gradients (Fig. 4) with a midzonal minimum (U-shaped gradients) was achieved by subdividing these gradients into their component parts with a "riverbed" approach. A circular, local-neighborhood maximum filter with a diameter of 15 pixels was applied to the original absorbance image (Fig. 4A and 4B), and the resulting image was simplified to three or four absorbance ranges in such a way that the midzonal minimum formed a continuous zone (Fig. 4C and 4D). The skeletonization of the plateau containing the lowest absorbance range yields the riverbeds. The riverbed was superimposed on the original image to evaluate the quality of the region-forming procedure (Fig. 4B). Comparison with the distribution of marker genes (enzymes) in adjacent sections allows for the classification of the areas enclosed by the contours as periportal or pericentral. To define the watershed of a midzonal maximum rather than the riverbed of a midzonal minimum, the riverbed procedure can be applied to the inverted grey values of the image.

RESULTS

For illustrative purposes, we only analyzed the images shown in Figs. 1, 2, 4 and 5. However, to obtain more reliable estimates, the results of more images and more sections can be summed according to established methods.[27]

Quantitative Graphical Description of a Portocentral Gradient in Gene Expression. Figure 1A shows the staining pattern of the

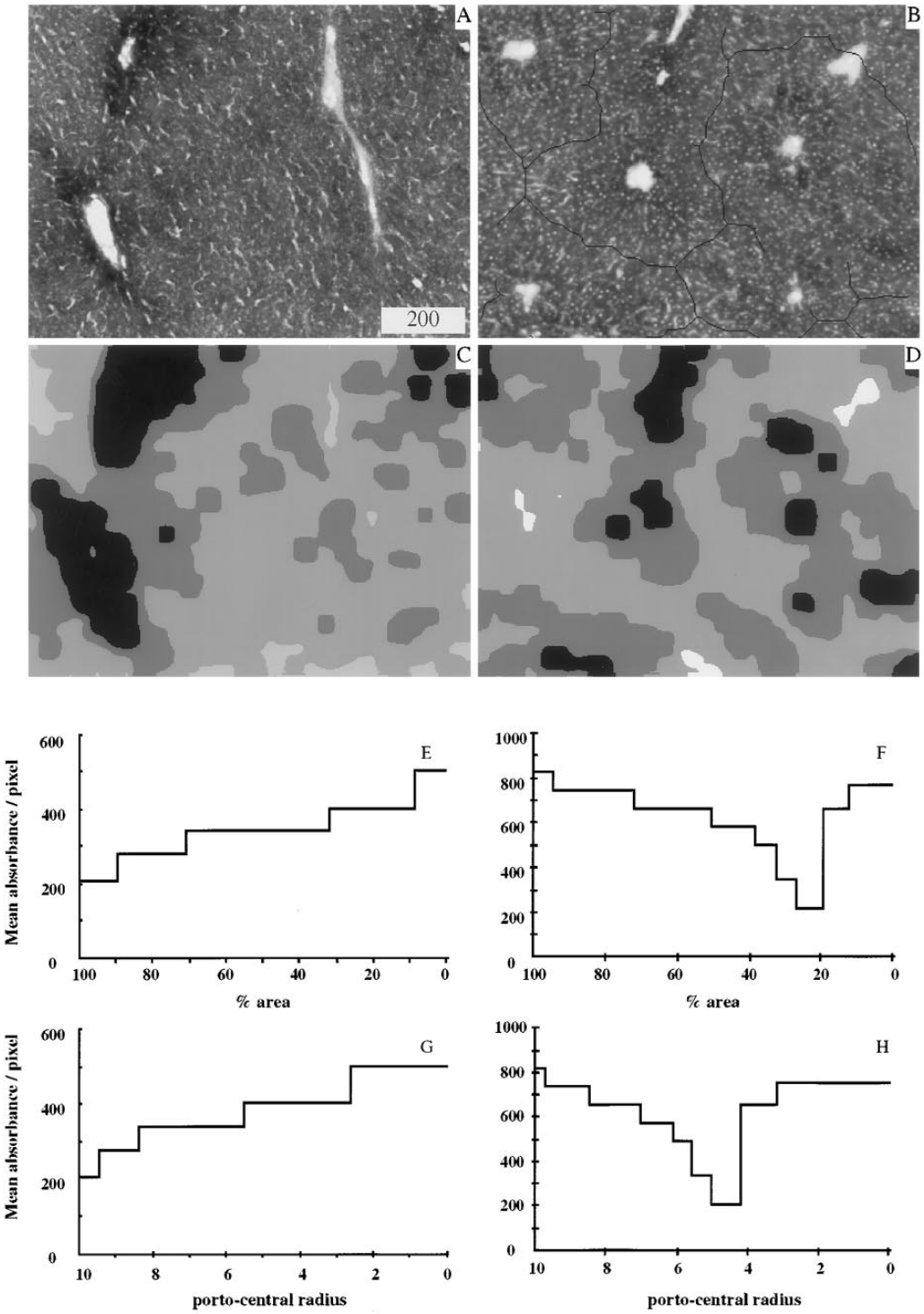

FIG. 4. Expression pattern of GDH enzyme activity in the liver of a fed and a 72-hour-fasted male rat. (A and B) The digital images of enzyme-histochemically stained sections. (C and D) The distribution of enzyme activity after application of a local neighborhood maximum filter to the original absorbance images (A and B) and simplification of the resulting image to four grey-value ranges. Skeletonization of the midzonal tracts of low enzyme activity yields the riverbed between the pericentral and the periportal regions with higher enzyme activity (B). (E and F) The frequency distribution of the pixels overlying hepatocytes with absorbance values in each of 10 grey-value ranges after determining the relative size of the periportal (left portion of profiles; 80% in [B]) and pericentral (right portion of profiles; 20% in [B]) zones, while (G and H) show the frequency distributions of pixels overlying hepatocytes with absorbance values corresponding to each of these grey-value ranges along the portocentral radius as derived from panels C and G. Note that (E, F, G, and H) are composed of frequency profiles separately determined in the periportal and pericentral zones and that their quantitative contribution (along the abscissa) is determined by the surface area of the periportal and pericentral zones as delineated by the riverbed. In (E-H) the portal tracts are located at the left end of the abscissa and on the right end of the central veins. *Bar* = 500 μm.

periportal enzyme carbamoylphosphate synthetase (CPS) in porcine liver.[28] After applying a Gaussian filter and subtracting the nonspecific background absorbance that is present in the portal tracts, the remaining absorbances were subdivided into grey-value ranges. For simplicity, only three ranges are visualized in Fig. 1B. The high, intermediate, and low absorbance ranges comprise 50%, 42%, and 8%, respectively, of the area in the image that is occupied by hepatocytes. The projection of the contours of the grey-value ranges illustrated in Fig. 1B on the image of Fig. 1A yields Fig. 1C. As expected, Fig. 1C shows that after application of the image-processing procedure, the highest absorbances are still solely found in the periportal area. The jagged contour lines between the successive grey-value ranges were found to follow cellular contours. They are not unique to our way of analyzing the images but are also seen in elaborate microbiochemical assays.[13,14] In Fig. 1D, we have determined the frequency distribution of the number of pixels in each of a number of successive grey-value ranges after dividing the total range between the highest and lowest specific absorbance over hepatocytes into 10 equal portions. By serially arranging these absorbance ranges in an ascending or de-

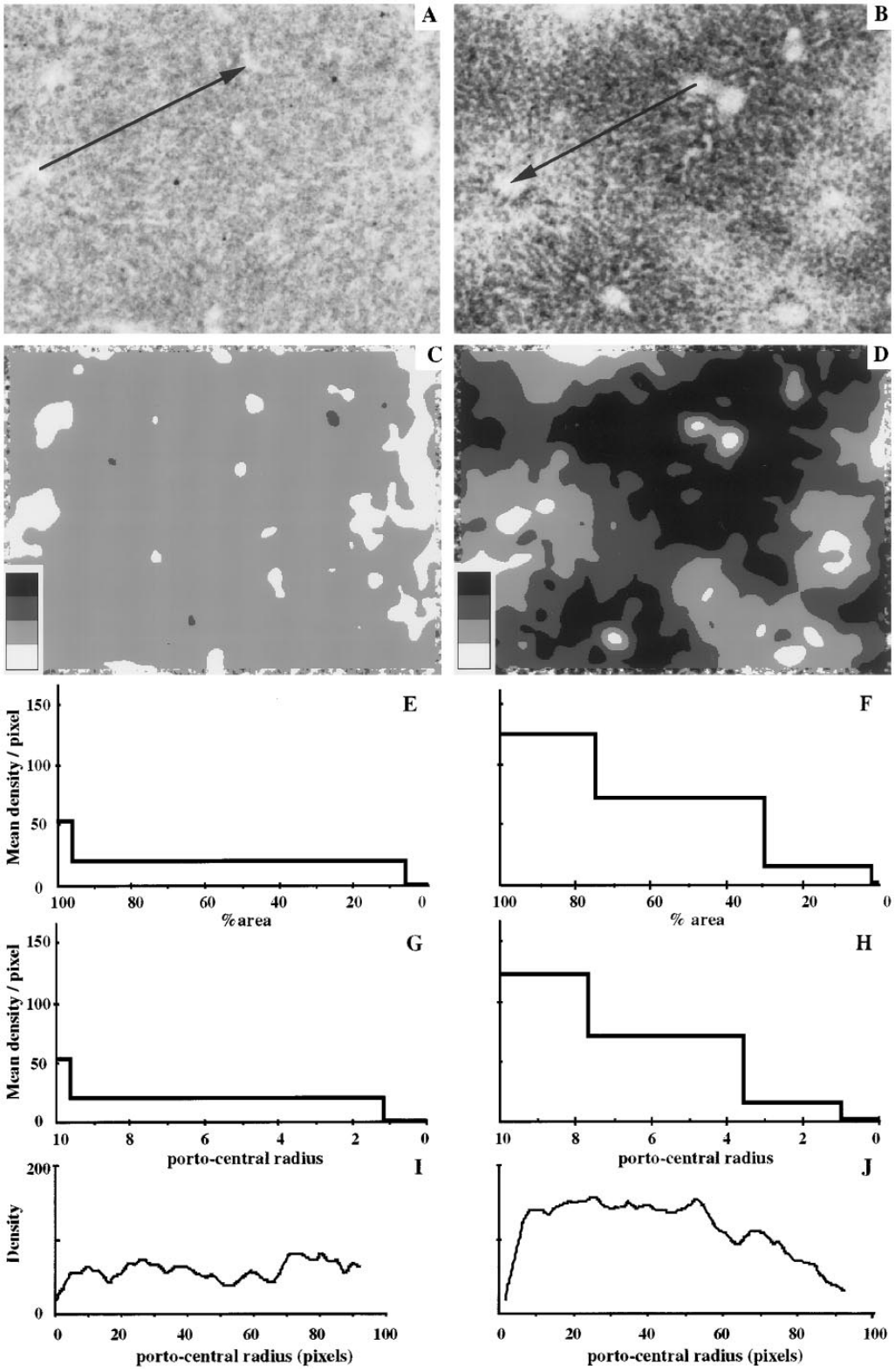

FIG. 5. Expression pattern of GDH mRNA in male rat liver before (A, C, E, and G) and after (B, D, F, and H) 72 hours of fasting. (A and B) Digital images of sections stained by *in situ* hybridization, (C and D) show the frequency distribution of pixels overlying hepatocytes with density values in each of 10 grey-value ranges in the section, (E and F) show the frequency distribution of pixels overlying hepatocytes with densities in each of these grey-value ranges along the portocentral radius, and (G and H) show the density along the portocentral radius indicated by the line in (A and B), respectively. Note that the signal is expressed in density units rather than in percentages to emphasize that the enhanced expression of GDH mRNA occurs predominantly in the periportal zone. In (C-J), the portal tracts are located at the left end of the abscissa and the central veins on the right end. *Bar* = 500 μm.

scending order, i.e., according to the *a priori* knowledge of the direction of the portocentral gradient, the frequency-distribution profile of hepatocytes with a particular absorbance in such a section is obtained. As can be seen (Fig. 1D), only eight absorbance ranges are shown. This is because we have grouped and averaged the upper three grey-value ranges, because together they occupy only 4% of the total number of pixels over hepatocytes.

In analyzing the frequency-distribution profile in Fig. 1D, we must realize that these data are obtained from sections, representing a surface area measurement. Panel D is therefore a graphical representation of the two-dimensional distribution pattern of CPS in the liver, with the position of the portal tract on the left end of the abscissa and that of the central vein on the right. The more typical linear distribution pattern, i.e., the gradient in the level of expression of CPS

along the portocentral radius, can be obtained by sampling a fair number of portocentral gradients in absorption along lines such as those drawn in Fig. 1B. The resulting gradients (without Gaussian smoothing) are shown in Fig. 1F and 1G and, after smoothing with a 7 × 11 pixel moving average procedure, in Fig. 1H and 1I. According to accepted procedures,[27] the summation of many such gradients would yield a graph that is comparable to Fig. 1E. However, the typical linear portocentral gradient can also be derived from panel D if we assume that liver lobules are uniform, more or less cylindrical or prismatic structures.[17] If this assumption is accepted, the portocentral radius can be approximated by taking the square root of the surface area, i.e., the parameter values on the abscissa in panel D. The border of the central vein, which is the longitudinal axis of the hepatic lobule,[4] is equivalent to position 0, and the border of the portal vein is equivalent to position 10 in such a calculation. The result of this computation is shown in Fig. 1E (for the applied formula, see Materials and Methods). Nevertheless, we have to stress that the data in Fig. 1D are directly derived from the section shown in Fig. 1A, whereas the data shown in Fig. 1E are derived from Fig. 1D on the assumption that lobules are prismatic structures. Future refinements of our models of the architecture of the structural unit of the liver may therefore modify the derived gradient in Fig. 1E to some extent.

Portocentral Gradients of Different Enzymes in the Same Liver. In mouse liver, the ornithine-cycle enzyme-CPS (Fig. 2A) is expressed in a wide periportal zone of hepatocytes. Its concentration is highest in the layer of hepatocytes that immediately surround the portal tract (the portal limiting plate,[29] levels out in the midlobular hepatocytes, and then declines towards the central vein, attaining very low levels in the hepatocytes directly surrounding this draining vessel. The expression pattern of the gluconeogenic enzyme phosphoenolpyruvate carboxykinase (PEP-CK) (Fig. 2B) is also typically periportal but is expressed in a much smaller zone, i.e., the decline in its hepatocellular content is localized more towards the portal end of the portocentral radius than that of CPS. Finally, the enzyme glutamine synthetase (GS) (Fig. 2C) is exclusively expressed in a 2-cell-wide rim of pericentral hepatocytes.[29] Figure 2D-F show the same images after subdividing the hepatocyte-specific absorbance into a high, an intermediate, and a low range. High levels of CPS are present in hepatocytes occupying 95% of the section surface area, high levels of PEP-CK in hepatocytes occupying 37% of the section surface area, and high levels of GS in hepatocytes occupying only 10% of the section surface area. Figure 2G–2I represent the frequency distribution of the number of pixels in each of the grey-value ranges, or a graphical representation of the two-dimensional distribution pattern of the three enzymes along the portocentral radius as shown in the images of Fig. 2A-2C. Information from the sections was used to determine the ascending or descending direction of the gradient in absorbance in these panels. To facilitate the comparison of the two-dimensional distribution pattern of the enzymes, the absorbance representing the maximum cellular concentration of each of the enzymes was set at 100%. In Fig. 2J-2L, the frequency distribution of the number of pixels in each of the grey-value ranges along the portocentral radius was calculated, again assuming that the hepatic lobules are cylindrical or prismatic structures. It is clear that the largest errors that potentially arise from this assumption are to be found near the axis of the lobule. Nevertheless, after correcting for the average size of the central veins, the number of layers of GS-positive hepatocytes surrounding the central veins in mice and rats (Fig. 2; panel L and not shown, respectively) corresponds very well with the number calculated by dividing the size of the GS-positive area with the length of the perimeter of the corresponding central vein.[30] With knowledge of the average tissue concentration of each of the enzymes, the data in Fig. 2J-2L can easily be recalculated to the cellular content of each enzyme in each hepatocyte along the portocentral radius. For such a calculation, it is necessary to know the number of hepatocytes that occupy the portocentral radius (10-12 hepatocytes in mouse liver).

A comparison between Fig. 2G-2I and Fig. 2J-2L clearly demon strates that the gradients in enzyme content as a function of the position of the hepatocyte on the (linear) portocentral radius underestimate the contribution of periportal cells to total liver content and overestimate that of the pericentral cells. This is particularly well-illustrated if the distribution of PEP-CK and GS are compared: their gradients along the portocentral radius are similar, but PEP-CK occupies a three- to fourfold larger area. This observation is in line with the well established fact that the terminal branches of the portal vein outnumber the central veins by the same factor[4,31,32] and with our argument that the lobule is an acceptable model of the structural unit of the liver.

Bipolar Portocentral Gradients of the Same Enzyme in the Same Liver. In the examples provided thus far, portocentral gradients could be directly extracted from the frequency distribution profile of the grey-value ranges because the portocentral gradient in gene expression was unidirectional (Fig. 5). However, several examples exist where maximum and minimum cellular enzyme content is not found in the hepatocytes surrounding either the portal tract or central vein but somewhere in between.[12,33] Our own studies of the distribution of glutamate dehydrogenase (GDH) have shown that in normally fed liver, the highest enzyme activity can be found in the pericentral hepatocytes (Fig. 4A).[24,34,35] However, upon prolonged fasting, the enzyme becomes induced in the periportal hepatocytes as well (Fig. 4B).[34,35] The resulting bipolar gradient with the lowest enzyme activity in midzonal hepatocytes is, of course, not seen when a frequency distribution profile of the absorbances overlying all hepatocytes is determined. However, delineation of the riverbed between the pericentral and periportal zones of high GDH activity (Fig. 4B and D) allows determination of their respective sizes. The zones delineated by the riverbeds can be identified unequivocally as periportal or pericentral by staining adjacent sections for periportal and pericentral marker enzymes (e.g., CPS or PEP-CK, and GS, respectively). Because the remaining gradients in the pericentral and periportal zones are unidirectional, the distribution profile of the grey-value ranges can be determined in each zone separately. The relative length of the abscissa of each of these two distribution profiles should represent the relative contribution of that zone to the total area of hepatocytes analyzed (Fig. 4B, 20% and 80% for the pericentral and periportal zones, respectively). Combination of the respective profiles will produce a quantitatively correct representation of the bipolar GDH activity gradient (Fig. 4F). The frequency distribution in the section (Fig. 4E and 4F) can be recalculated to the frequency distribution along the portocentral radius (Fig. 4G and 4I), as shown in the previous paragraphs.

If a midzonal maximum rather than a minimum is seen, for example in glucokinase in male rats,[33] the "riverbed" of the inverted grey values of the image has to be determined to resolve both components of the portocentral gradient.

Portocentral Gradients of the Same Enzyme in Different Livers. The frequency-distribution profiles are very useful tools to evaluate the effects of a particular treatment on the zonal distribution of a gene product. Figure 5 shows an image of the expression of GDH mRNA in fed male rat liver (Fig. 5A) and upon three days of fasting (Fig. 5B).[35] Because of the local heterogeneity in grey values, these *in situ* hybridization images were treated somewhat differently from the preceding immuno- and enzyme-histochemical data. If the portocentral gradient could be derived directly from the frequency distribution of the grey values, the gradient would be artificially steep, because relatively low grey values in regions with an overall high density would move downward in the gradient. For that reason, we applied a Gaussian filter (s_x and s_y: 15 pixels) before dividing the sections in equidensity zones. Subsequently, we measured the average density in each of these zones, using the original image. A comparison of the pictures shows that the distribution of GDH mRNA in fed male liver is almost homogeneous, whereas upon fasting, a pronounced increase in hepatocellular GDH mRNA content is observed in the periportal hepatocytes.[35] The density gradients of both images are shown in Fig. 5C and 5D, and the linear portocentral gradient in cellular GDH mRNA content is shown in Fig. 5E and 5F. For comparison, the density along the lines drawn in Fig. 5A and 5B is given in Fig. 5G and 5H, and after smoothing with a 7×11 pixel moving average procedure, in Fig. 5I and 5J. By using the average density values as such rather than expressing them as a percentage, it can be seen directly that fasting affects GDH mRNA expression in the periportal hepatocytes only. Because the area under the curve represents the total hepatic content of GDH mRNA, these data can be combined with absolute (molar) measurements in homogenates to calculate the cellular concentration of GDH mRNA in each hepatocyte along the portocentral radius.

Our graphical description of portocentral gradients in hepatic enzyme contents also allows a quantitative comparison of the pattern of expression of the same gene in different species. For example, comparison of the expression pattern of CPS in pig and mouse liver (Fig. 1A, 1B, 1D, and 1E; and Fig. 2A, 2D, 2G, and 2J) shows that the midlobular plateau in CPS content, which is highly characteristic for mouse liver, is not present in pig liver.

CONCLUSION

Quantitative evaluation of zonal heterogeneity in hepatic enzyme content is often based on spot measurements in the periportal, intermediate, and pericentral zones of the liver. These spot measurements usually represent absorbance values of precipitates produced by enzyme-histochemical reactions on cryostat sections,[10,36,37] or biochemical analyses of enzyme activities in 6 to 10 samples that together form narrow strips of tissue that comprise the portocentral radius.[11,12,14-16,38,39] The data generated by such enzyme-histochemical or microbiochemical approaches accurately reflect local differences in enzyme content. On the other hand, the distribution pattern of such enzymes as seen in sections only locally matches either the classical lobular or acinar distribution pattern, making it difficult to interpret the data in the context of hepatic architecture. Moreover, even though the laborious study of Takahashi et al.[40] has shown that the distance between the afferent and efferent vessels in the liver (the length of the hepatic sinusoids) is the most homogeneous of any organ in the body, the ratio between the shortest and the longest 2.5% of the sinusoidal routes is still two. Because of these local variations in the diameter of the lobule, the effects of which add up with the previously cited tortuosity of the lobules, the distance between the portal and central veins as seen in sections can vary substantially, ensuing a similar variation in the steepness of the portocentral gradient in enzyme content if the portocentral radius is normalized to 100%, as is often done.[11,16,27,38] For that reason, determination of gradients in hepatocellular content of gene products along the portocentral radius as found in sections is not easily accessible to automatic image analysis if such an analysis has to start with the identification of the portal and central ends of the gradient.[41] We, therefore, developed a time-efficient approach that takes the entire image into account rather than a selected portion of it. By summarizing the data from several sections and/or animals according to established procedures,[27] confidence intervals for the findings can be established. The approach generates a quantitative description of the relation between the enzymic phenotype of hepatocytes and their position on the portocentral radius. Furthermore, the portocentral radius is normalized in this graphical description of portocentral gradients in gene expression. A major indirect advantage of the present approach, which is based on image processing for determining the prevalence of hepatocytes with defined cellular concentrations of a particular gene product, is that the outcome can be directly related to biochemical measurements in total tissue homogenates. In fact, the basis of the method presented here was suggested by the way De Duve et al. expressed enzyme distributions that resulted from differential centrifugation of homogenates in histogram form.[42]

REFERENCES

1. Jungermann K, Katz N. Functional specialization of different hepatocyte populations. Physiol Rev 1989;69:708-764.
2. Meijer AJ, Lamers WH, Chamuleau RAFM. Nitrogen metabolism and ornithine cycle function. Physiol Rev 1990;70:701-748.
3. Gebhardt R. Metabolic zonation of the liver: regulation and implications for liver function. Pharmacol Ther 1992;53:275-354.
4. Matsumoto T, Kawakami Mà. The unit-concept of liver parenchyma—a reevaluation based on angioarchitectural studies. Acta Pathol 1982; 32:285-314.
5. Lindros KO. Digitonin-collagenase perfusion for efficient separation of periportal and perivenous hepatocytes. Biochem J 1985;228:757-760.
6. Quistorff B, Romert P. High zone-selectivity of cell permeabilization following digitonin-pulse perfusion of rat liver. A re-interpretation of the microcirculatory zones. Histochemistry 1989;92:487-498.
7. Rappaport AM. The microcirculatory acinar concept of normal and pathological hepatic structure. Beitr Pathol Bd 1976;157:217-243.
8. McCuskey RS. The hepatic microvascular system. In: Arias IM, Boyer JL, et al. The Liver: Biology and Pathobiology. 3rd Ed. New York: Raven, Ltd., 1994:1089-1106.
9. Görgens HW, Hildebrand R, Haubitz I. Distribution pattern of alanine aminotransferase activity in rat liver. Histochemistry 1988;88:383-386.
10. Chikamori K, Araki T, Yamada MO. Pattern analysis of heterogenous distribution of succinate dehydrogenase in single rat hepatic lobules. Cell Mol Biol 1985;31:217-222.
11. Teutsch HF. A new sample isolation procedure for microchemical analysis of functional liver cell heterogeneity. J Histochem Cytochem 1986; 34:263-267.
12. Teutsch HF. Quantitative histochemical assessment of regional differences in hepatic glucose uptake and release. Histochemistry 1985;82: 159-164.

13. Teutsch HF, Chilko DM. Use of 3D-computer graphics for imaging of distribution of hepatic metabolites. Histochemistry 1986;84:396-400.
14. Teutsch HF, Altemus J, Gerlach-Arbeiter S, Kyander-Teutsch TL. Distribution of 3-hydroxybutyrate dehydrogenase in primary lobules of rat liver. J Histochem Cytochem 1992;40:213-219.
15. Hildebrand R, Fuchs C. Microbiochemical investigation on diurnal rhythmic changes of the activities of the lactate dehydrogenase in the periportal and perivenous zones of the acinus of the rat liver. Histochemistry 1984;81:477-483.
16. Ebert S, Hildebrand R, Haubitz I. Sinusoidal profiles of lactate dehydrogenase activity in rat liver. Histochemistry 1987;87:371-375.
17. Braus H. Mitteilungen über Lebermodelle. Anat Anz 1921;54:119-124.
18. Gaasbeek Janzen JW, Lamers WH, Moorman AFM, de Graaf A, Los JA, Charles R. Immunohistochemical localization of carbamoylphosphate synthetase (ammonia) in adult rat liver. J Histochem Cytochem 1984; 32:557-564.
19. Moorman AFM, de Boer PAJ, Vermeulen JLM, Lamers WH. Practical aspects of radio-isotopic in situ hybridization on RNA. Histochem J 1993;25:251-260.
20. Jonker A, de Boer PAJ, van den Hoff MJB, Lamers WH, Moorman AFM. Toward a quantitative in situ hybridisation method. Quantitative in situ detection of CPS mRNA in rat intestinal epithelium model system. J Histochem Cytochem 1997;45:413-423.
21. Nibbering PH, Marijnen JGJ, Raap AK, Leij PCJ, van Furth R. Quantitative study of enzyme immunocytochemical reactions performed with enzyme conjugates immobilized on nitrocellulose. Histochemistry 1986; 84:538-543.
22. Pool CW, Madlener S, Diegenbach PC, Sluiter AA, van der Sluis P. Quantification of antiserum reactivity in immunocytochemistry. Two methods for meauring peroxidase activity on antigen-coupled beads incubated according to an immunocytoperoxidase method. J Histochem Cytochem 1984;9:921-928.
23. Van Noorden CJF, Frederiks WM. Enzyme Histochemistry: A Laboratory Manual of Current Methods. Oxford: Oxford University Press, 1992.
24. Jonker A, Geerts WJC, Charles R, Lamers WH, van Noorden CJF. Image analysis and image processing as tools to measure initial rates of enzyme reactions in sections: distribution patterns of glutamate dehydrogenase activity in rat liver lobules. J Histochem Cytochem 1995;43:1027-1034.
25. Rogers AW. The collection of data from autoradiographs. In: Rogers AW, ed. Techniques of Autoradiography. Vol. 3. Amsterdam: Elsevier Biomedical Press, 1979:201-228.
26. Ten-Kate TT, van Balen R, Smeulders AWM, Groen FCA, den Boer GA. SCIL-Aim: a multi-level interactive image processing environment. Pattern Recognition Lett 1990;11:429-441.
27. Teutsch HF. Chemomorphology of liver parenchyma. Progr Histochem Cytochem 1981;14:1-88.
28. Wagenaar GTM, Geerts WJC, Chamuleau RAFM, Deutz NEP, Lamers WH. Lobular patterns of expression and enzyme activities of glutamine synthase, carbamoylphosphate synthase and glutamate dehydrogenase during postnatal development of the porcine liver. Biochim Biophys Acta 1994;1200:265-270.
29. Wagenaar GTM, Moorman AFM, Chamuleau RAFM, Deutz NEP, de Gier-de Vries C, de Boer PAJ, Verbeek FJ, et al. The vascular branching pattern and zonation of gene expression in the mammalian liver. Anat Rec 1994;239:441-452.
30. Gebhardt R, Williams GM. Glutamine synthetase and hepatocarcinogesis. Carcinogenesis 1995;16:1673-1681.
31. Pfuhl W. Die Leber. In: von Möllendorf W, ed. Handbuch Der Mikroskopischen Anatomie des Menschen. Vol. 5. Berlin: Springer, 1932: 235-425.
32. Rappaport AM. The microcirculatory hepatic unit. Microvasc Res 1973; 6:212-228.
33. Teutsch HF, Lowry OH. Sex specific regional differences in hepatic glucokinase activity. Biochem Biophys Res Commun 1982;106:533-538.
34. Lamers WH, Gaasbeek Janzen JW, Moorman AFM, Charles R, Knecht E, Martinez-Ramon A, Hernandez-Yago J, et al. Immunohistochemical localization of glutamate dehydrogenase in rat liver; plasticity of the distribution during development and with hormone treatment. J Histochem Cytochem 1988;36:41-47.
35. Geerts WJC, Verburg M, Jonker A, Boon L, Charles R, van Noorden CJF, Lamers WH. Independent regulation of GDH expression in periportal and pericentral hepatocytes of male and female rats upon starvation; in press.
36. Jonges GN, van Noorden CJF, Lamers WH. *In situ* kinetic parameters of glucose-6-phosphatase in the rat liver lobulus. J Biol Chem 1992; 267:4878-4881.
37. Jonges GN, van Noorden CJF. *In situ* kinetic parameters of glucose-6-phosphate dehydrogenase and phosphogluconate in different areas of the liver acinus. Histochem J 1989;21:585-594.
38. Maly IP, Sasse D. Microquantitative analysis of the intra-acinar profiles of glutamate dehydrogenase in rat liver. J Histochem Cytochem 1991; 39:1121-1124.
39. Chamlian A, Benkoel L, Bongrand P, Gulian JM, Brisse J. Quantitative histochemical study of glucose-6-phosphatase in periportal and perivenous human hepatocytes. Cell Mol Biol 1991;37:183-190.
40. Takahashi T. Lobular structure of the human liver from the viewpoint of hepatic vascular architecture. Tohoku J Exp Med 1970;101:119-140.
41. Hildebrand R, Sleicher A. Image analysis of the histochemical demonstration of glucose-6-phosphatase activity in rat liver. Histochemistry 1986;86:181-190.
42. De Duve C. Exploring cells with a centrifuge. Science 1975;189:186-194.